

The Magnetic Stability of Spin-Dependent Tunneling Devices

S. Gider,* B.-U. Runge, A. C. Marley,† S. S. P. Parkin‡

The tunneling resistance between two ferromagnetic metal layers that are separated by a thin insulator depends on the relative orientation of the magnetization \mathbf{M} of each layer. In a memory device, independent switching of the magnetically soft layer is achieved by making the other layer either exchange-biased or magnetically hard. The repeated reversal of \mathbf{M} of the soft layer by field cycling can demagnetize the other magnetically hard layer and thus erase the tunnel junction's memory. The \mathbf{M} of exchange-biased structures was stable at least to 10^7 cycles, whereas in hard structures, \mathbf{M} generally decayed logarithmically with the number of field cycles. The decay was very sensitive to the thickness of the hard layer and the composition of the soft layer. However, no decay was observed when the moment reversal was accomplished by coherent rotation, establishing that demagnetization results from the formation and motion of domain walls in the soft layer during field cycling.

Magnetic thin films are currently the basis of information storage technology (1). Generally, disk media are magnetically hard alloys of Co, and read/write sensors are predominantly soft alloys of Ni and Fe, such as Permalloy ($\text{Ni}_{81}\text{Fe}_{19}$). Before the introduction of charge memory devices, such as dynamic RAM, magnetic thin films were considered as an alternative to magnetic core memories (2). The discovery of magnetoresistive (MR) effects that are much greater in heterostructures (3, 4) than MR effects in homogenous films has led to a renewed interest in magnetic memory devices. Magnetic memory is inherently nonvolatile and does not require periodic refreshing, as do charge memory devices. Over the last decade, the spin-valve heterostructure has been extensively studied for disk and memory applications (5). A spin valve is composed of two ferromagnetic (FM) layers (such as Permalloy or Co) with a spacer layer of a nonmagnetic conductor (typically Cu). In contrast, the spacer layer in a tunnel junction is a thin insulator (6). Recently, tunnel junctions have been realized with an MR effect that is greater than the MR effect in spin valves (7), 25% versus 10% for a simple spin valve (8). In tunnel junctions, the large MR is a consequence of the difference in the density of states for tunneling (9). When the \mathbf{M} 's of the two FM layers are antiparallel, the probability of electron tunneling is low and the resistance R is high

because for a given electron spin state in one layer, there are a small number of empty electron states with the same spin in the other layer. Inversely, when the two \mathbf{M} 's are parallel, the tunneling probability is high and R is low.

The antiparallel and parallel \mathbf{M} arrangements in a tunnel junction may represent the two states of a bit. Reading the information only requires a measurement of R . Writing the information involves a switching of \mathbf{M} for one layer, ideally without affecting \mathbf{M} for the reference layer. Coupling between the layers may eventually demagnetize the reference layer and effectively erase the memory of the tunnel junction. A magnetic tunnel junction memory requires a reference layer that is stable over millions of \mathbf{M} reversals of the free layer. To stabilize the reference layer, its hysteresis loop can be shifted away from the zero field by exchange biasing; \mathbf{M} of the reference layer is pinned to an adjacent antiferromagnetic (AF) layer through an exchange interaction, which effectively acts as an internal field on the reference layer and must be overcome in order to switch the layer. The hysteresis loop of the reference layer can also be widened or magnetically hardened by alloying it. We studied the stability of exchange-biased and hard layers by following \mathbf{M} of the reference layers after switching \mathbf{M} of the free layer. Whereas \mathbf{M} of an exchange-biased reference layer is stable at least to 10^7 cycles, \mathbf{M} of a hard reference layer generally decays logarithmically with the number of cycles and is eventually completely demagnetized.

All of the samples were formed by dc magnetron sputtering in 10^{-3} torr of Ar after reaching an ultrahigh vacuum of 10^{-9} torr. The tunneling barrier is composed of Al_2O_3 , which is formed by depositing metallic Al

followed by plasma oxidation in 0.1 torr of O_2 . Because only the Al thickness (not the actual Al_2O_3 thickness) is known, the barrier thickness is given as the Al thickness. (The thickness typically increases by $\sim 30\%$ after plasma oxidation.) The samples were formed on Si(100) wafers with a 5000 Å-thick SiO_2 layer for electrical isolation between junctions. A series of in situ contact masks defined 10 junctions, each $6400 \mu\text{m}^2$ in area, with leads and contacts for four-point resistance measurements and simultaneously defined 1.5 mm by 6.0 mm areas for \mathbf{M} measurements. Thus, complementary measurements were possible on the same structure, albeit on different areas of the structure. All of the measurements were performed at room temperature.

Measurements of \mathbf{M} and MR for an exchange-biased structure and a hard layer structure are shown in Fig. 1. In the first structure, the reference layer of Co is exchange-biased by MnFe, and its hysteresis loop is shifted toward positive field (Fig. 1A). (The direction of the exchange bias is defined by an external field during the formation.) In the hard layer structure, the reference layer of $\text{Co}_{75}\text{Pt}_{12}\text{Cr}_{13}$ switched symmetrically at a higher field of $\sim 2000 \text{ Oe}$ as compared to the free Co layer, which switched at a field of $\sim 50 \text{ Oe}$ (Fig. 1C). As shown in the corresponding MR curves (Fig. 1, B and D), both structures show a maximum in R near zero field, where \mathbf{M} 's of the free and reference layers are antiparallel, and a minimum in R at high fields, where \mathbf{M} 's of the two layers are parallel. In general, we have been able to achieve higher MR with an exchange-biased layer than with a hard layer, mainly because the exchange-biased layer has a more uniform \mathbf{M} than the hard layer.

To simulate the writing of bits, we repeatedly reversed \mathbf{M} of the free layer with a magnetic field that was large enough to saturate the free layer but was too small to reverse the reference layer ($\pm 100 \text{ Oe}$ for the exchange-biased structure and $\pm 200 \text{ Oe}$ for the hard-layer structure). The remanent state of the reference layer was then sensed by \mathbf{M} . (Alternatively, the state could be sensed by R .) A marked difference in the stability of \mathbf{M} of exchange-biased and hard layers is evident in the decay curves of Fig. 2. The \mathbf{M} of the exchange-biased layer was stable for at least 10^7 cycles, which is equivalent to about one write cycle per second for 1 year. In contrast, \mathbf{M} of the hard layers had a slow logarithmic decay toward demagnetization. The initial form of the decay can be well described by $M/M_R \approx 1 - [\log(N/N_0)]^2$, where M_R is the initial remanent M of the reference layer, N is the number of cycles, and N_0 is an adjustable parameter. The decay is independent of the frequency of the cycling at least to 10 kHz, as verified by cycling at 500 and 50 Hz

IBM Research Division, Almaden Research Center, 650 Harry Road, K11/D2, San Jose, CA 95120-6099, USA.

*Present address: IBM Storage Systems Division, 5600 Cottle Road, N17A/142, San Jose, CA 95193, USA.

†Present address: IBM Storage Systems Division, 5600 Cottle Road, E44/15, San Jose, CA 95193, USA.

‡To whom correspondence should be addressed. E-mail: parkin@almaden.ibm.com

REPORTS

in the electromagnet and by cycling slowly in the superconducting magnet (but only for up to ~ 1000 cycles). Frequency independence implies that the effect is not due to eddy current heating. However, when the extrinsic cycling time approaches the intrinsic magnetic-switching time (on the order of nanoseconds), the decay is expected to become frequency-dependent.

The decay was strongly dependent on the thickness of the hard layer (Fig. 2). Increasing the thickness from 50 to 100 Å delays the demagnetization by one order of magnitude in the number of cycles. The rate of decay continued to decrease for thicknesses at least to 200 Å, although there was no observable change in the coercive fields of the hard layers beyond ~ 100 Å. For increasing thickness of the hard layer, the coercive fields of the free layers increased from 20 Oe with a 50 Å hard layer to 54 Oe with a 200 Å hard layer. The thicker hard layers may be rougher and may produce more pinning sites for magnetic domains in the free layer, thereby increasing the coercivity of the free layer.

To further explore the mechanism for the decay, a hard layer structure was cycled for different field amplitudes. A sudden onset of decay (Fig. 3) occurred when the field amplitude exceeded the coercive field (~ 50 Oe) of the free layer. The decay was weakly dependent on the amplitude beyond the threshold,

slower for ± 75 Oe than for ± 200 Oe, suggesting that a field of ± 75 Oe does not completely rotate M of the free layer. The observation that a homogenous hard layer alone is stable even when cycled with ± 200 Oe provides additional evidence that the decay of the hard layer is induced by coupling with the free layer. The effect is therefore distinct from magnetization creep, which is the slow formation of domains of opposite M in homogenous layers that are cycled with a field along the magnetic hard axis and a constant field along the easy axis (10).

Coupling between thin FM layers has been studied extensively, both experimentally and theoretically. If the layers are separated by a conductor, there is an exchange coupling that oscillates between FM and AF as a function of the conductor thickness (4, 11). In addition, there is roughness-induced magnetostatic coupling, which dominates the interaction between FM layers that are separated by an insulator (12). Such "orange peel" coupling arises from correlated roughness between the two layers. Along the interface, the magnetic dipole interaction will favor the alignment of M in a peak of one layer with M in an adjacent trough in the other layer. The coupling is analogous to permanent magnets in a line favoring an arrangement wherein opposite poles are next to each other and the M 's are all parallel. The Néel theory assumes

the layers to be of a single domain; however, the domain structure cannot be ignored in our samples with characteristic dimensions of millimeters.

Because the free layer is the last layer deposited in the structure, its roughness is considerably affected by the underlying Al_2O_3 and hard layers. Furthermore, because Al_2O_3 is an essentially inert insulator, chemical interaction with the metallic free layer is not significant and is unlikely to affect the roughness correlations. By replacing the free layer with a different material of the same net M , the roughness and hence the orange peel coupling are not affected, but the domain structure can be altered. A substantial increase in stability was observed when the free layer of Co was replaced with an alloy of Ni and Fe, specifically $\text{Ni}_{40}\text{Fe}_{60}$. This alloy has the same M and coercive field as Co. However, after 10^5 cycles, a hard layer of 100 Å $\text{Co}_{75}\text{Pt}_{12}\text{Cr}_{13}$ was completely demagnetized when it was coupled to a free layer of 150 Å

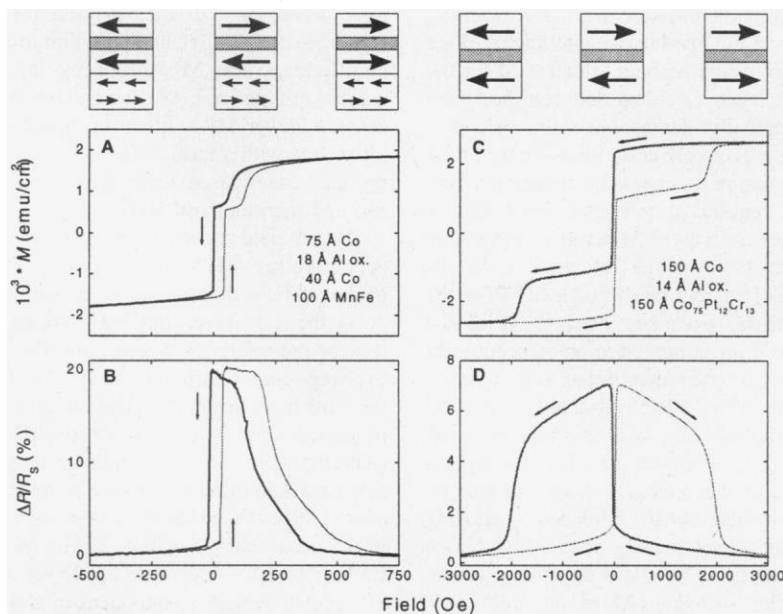


Fig. 1. (A and C) M and (B and D) MR loops of exchange-biased and hard layer structures, respectively. M is measured with a radio frequency superconducting quantum interference device, which senses the total moment and thus superimposes the hysteresis loops of the two layers. The MR ratio $\Delta R/R_s$ is defined as $[R(H) - R_s]/R_s$, where $R(H)$ is the resistance at a particular field H and R_s is the resistance at saturation, where the M 's of the two layers are parallel. The corresponding M directions are shown in schematic cross sections of each structure (the shaded area represents the insulating barrier); the actual layer thicknesses and compositions are listed in the panels of the M loops (A and C). In the exchange-biased structure, the AF layer of MnFe is represented by a layer with alternating M directions. The arrows in the loops indicate the direction of the field sweep. Thick curves represent the field swept from positive to negative fields, and thin curves represent the field swept from negative to positive fields. Electromagnetic unit, emu.

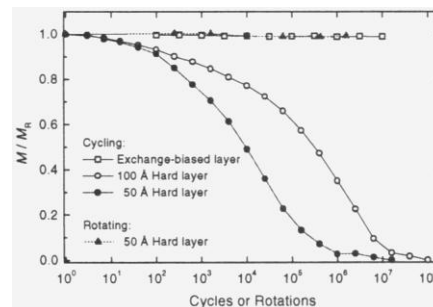


Fig. 2. The change in remanent M of the reference layers with numbers of field cycles (± 200 -Oe varying applied field) or rotations (200-Oe fixed field) of the free layers, plotted on a logarithmic scale. The curves are normalized by the remanent magnetization M_R , set at 5000 Oe before cycling or rotating. The error in the magnetization measurement is approximately the size of the plotted points. (In order to reach a million cycles within a reasonable time, the samples are cycled in a resistive coil that is part of a resonant circuit tuned to 10 kHz).

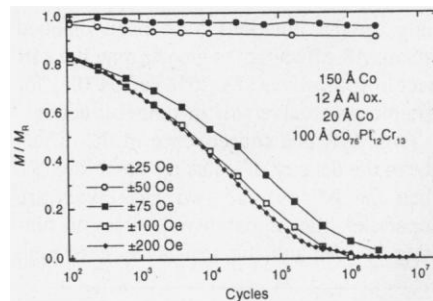


Fig. 3. The dependence of the decay on the amplitude of cycling. The 20 Å of Co at the interface between the $\text{Co}_{75}\text{Pt}_{12}\text{Cr}_{13}$ hard layer and the Al_2O_3 tunneling barrier enhances the magnetoresistance but does not alter the threshold for decay. The actual layer thicknesses and compositions are listed in the figure.

Co, but the hard layer only decayed to 65% of its original remanence when it was coupled to 150 Å Ni₄₀Fe₆₀. With a thicker Co₇₅Pt₁₂Cr₁₃ hard layer of 150 Å and a Ni₄₀Fe₆₀ free layer, the structure was stable to at least 10⁷ cycles.

A possible explanation of the decay of the hard layer moment with cycling of the free layer moment is that the decay results from the demagnetizing field at the hard layer that is associated with domain walls in the free layer. The strength of the demagnetizing field will depend on the detailed structure of the domain walls in the free layer. These domain walls are likely to be different in Co and NiFe because of their different anisotropies. Through their associated demagnetizing fields, the motion of the domain walls during the reversal of **M** will demagnetize the moment of the hard layer. To test this explanation, we reversed the moment of the free layer by a coherent rotation of its magnetic moment without the formation of domain walls; at 10 Hz, the sample was rotated about its surface, normal in a fixed homogenous magnetic field of 200 Oe, which was applied in the plane of the sample. The magnitude of the fixed field was chosen to be sufficiently larger than the coercivity of the free layer to ensure coherent rotation.

The change in the remanent **M** of the hard layer is shown by a comparison of the results that are obtained by repeatedly rotating a sample with a 50 Å-thick hard layer and by cycling the field on the same sample (Fig. 2). For up to 1.6 × 10⁶ rotations, there is no decay of the hard layer remanent moment within experimental error, whereas the hard layer was completely demagnetized after the same number of cycles. This result clearly shows that the formation and motion of domain walls play an important role in the observed demagnetization process.

The magnitude and spatial extent of the demagnetizing fields from the domain walls in the free layer must depend on the detailed magnetic structure of the domain walls. Thus, it would not be surprising if the **M** decay (which we have observed) depends on the thickness of the hard layer as well as on the composition of the free layer because, for example, the width of the domain wall and, consequently, the strength of the demagnetizing field would also depend on both **M** and the magnetic anisotropy of the free layer. However, it is difficult to probe the domain wall structure. In a magnetic force microscope, the stray field from the magnetic tip disturbs the structure of the magnetically soft free layers in our structures. Instead, we have carried out plan-view Lorentz transmission electron microscopy on structures formed on 500 Å-thick Si₃N₄ membranes. Although some differences are observed between the Co and NiFe layers, it is difficult to resolve the detailed magnetic structure of the domain walls because only the in-plane component of **M** produces

contrast. Electron holography will likely provide the additional information that is necessary to understand the details of the domain walls. Further investigations will extend the current study of large-area films to small patterned structures on the scale of domains.

References and Notes

1. J. L. Simonds, *Phys. Today* **48**, 26 (1995); K. G. Ashar, *Magnetic Disk Drive Technology: Heads, Media, Channel, Interfaces, and Integration* (Institute of Electrical and Electronics Engineers, New York, 1997).
2. A. Chiu *et al.*, *IBM J. Res. Dev.* **40**, 283 (1996).
3. G. Binasch, P. Grünberg, F. Saurenbach, W. Zinn, *Phys. Rev. B Condens. Matter* **39**, 4828 (1989); M. N. Baibich *et al.*, *Phys. Rev. Lett.* **61**, 2472 (1988).
4. S. S. P. Parkin, N. More, K. P. Roche, *Phys. Rev. Lett.* **64**, 2304 (1990).
5. B. Dieny *et al.*, *Phys. Rev. B Condens. Matter* **43**, 1297 (1991); S. S. P. Parkin, *Phys. Rev. Lett.* **71**, 1641 (1993); J. C. S. Kools, *IEEE Trans. Magn.* **32**, 3165 (1996); For an explanation and demonstration of the giant MR/spin-valve head, see www.research.ibm.com/research/gmr.html.

6. M. Jullière, *Phys. Lett. A* **54**, 225 (1975).
7. J. S. Moodera, L. R. Kinder, T. M. Wong, R. Meservey, *Phys. Rev. Lett.* **74**, 3273 (1995); S. S. P. Parkin, R. E. Fontana, A. C. Marley, *J. Appl. Phys.* **81**, 5521 (1997); W. J. Gallagher *et al.*, *ibid.*, p. 3741; J. M. Daughton, *ibid.*, p. 3758.
8. A 21% effect is possible with a more complicated spin-valve structure. See W. F. Egelhoff *et al.*, *ibid.* **78**, 273 (1995).
9. J. C. Slonczewski, *Phys. Rev. B Condens. Matter* **39**, 6995 (1989).
10. W. Kayser, *IEEE Trans. Magn.* **3**, 141 (1967).
11. S. S. P. Parkin, R. Bhadra, K. P. Roche, *Phys. Rev. Lett.* **66**, 2152 (1991).
12. L. Néel, *C. R. Hebd. Seances Acad. Sci.* **255**, 1545 (1962); *ibid.*, p. 1676.
13. We thank S. A. Crooker, P. P. Crooker, and M. Scheinfein for helpful discussions. We also thank R. E. Dunin-Borkowski, M. R. McCartney, and D. J. Smith for Lorentz microscopy studies. B.-U.R. thanks the Alexander von Humboldt Foundation, Germany, for a Feodor Lynen Fellowship.

5 December 1997; accepted 26 June 1998

Evidence of Soft-Mode Quantum Phase Transitions in Electron Double Layers

Vittorio Pellegrini, Aron Pinczuk, Brian S. Dennis, Annette S. Plaut, Loren N. Pfeiffer, Ken W. West

Inelastic light scattering by low-energy spin-excitations reveals three distinct configurations of spin of electron double layers in gallium arsenide quantum wells at even-integer quantum Hall states. The transformations among these spin states appear as quantum phase transitions driven by the interplay between Coulomb interactions and Zeeman splittings. One of the transformations correlates with the emergence of a spin-flip intersubband excitation at vanishingly low energy and provides direct evidence of a link between quantum phase transitions and soft collective excitations in a two-dimensional electron system.

A two-dimensional (2D) electron gas, when subjected to a perpendicular magnetic field B_{\perp} , exhibits remarkable behavior that follows from the quantization of the in-plane kinetic energy into Landau levels, the Zeeman splitting of different spin states, and the impact of strong Coulomb interactions. The quantum Hall effects occur when changes in B_{\perp} or electron density, or both, cause the Fermi energy to sweep across spin-split Landau levels ($l-3$). Quantum Hall states are distinct phases of the 2D electron gas displaying precise quantization of the Hall effect and

vanishing longitudinal magnetoresistance. They are observed at integer and some fractional values of Landau-level filling factor $\nu = n2\pi l_{\text{B}}^2$. Here, n is the areal electron density and $l_{\text{B}} = (hc/2\pi eB_{\perp})^{1/2}$ is the magnetic length. c is the speed of light, \hbar is Planck's constant, and e is the electron charge. Experimental and theoretical studies of quantum Hall phenomena have uncovered some of the more intriguing behavior in contemporary physics. Notable examples are low-temperature quantum phase transitions tuned by the external magnetic field [for recent reviews see (4-7)]. Evidence of phase transformations appears in magnetotransport as anomalies in quantum Hall states. In current theories, the transformations are triggered by low-energy collective excitations of quantum Hall states. Within this framework, the softening of a low-energy mode induces an instability in which the 2D electron system changes quantum ground state by incorporating properties associated with the excitation ($\delta-12$).

V. Pellegrini, Bell Laboratories, Lucent Technologies, Murray Hill, NJ 07974, USA, and Scuola Normale Superiore and Istituto Nazionale per la Fisica della Materia, Pisa, Italy. A. Pinczuk, Bell Laboratories, Lucent Technologies, Murray Hill, NJ 07974, USA, and Departments of Physics and Applied Physics, Columbia University, New York, NY 10027, USA. B. S. Dennis, L. N. Pfeiffer, K. W. West, Bell Laboratories, Lucent Technologies, Murray Hill, NJ 07974, USA. A. S. Plaut, Department of Physics, University of Exeter, Exeter EX4 4QL, UK.